

Lili Eszter Laczák, György Károlyi

60(4), pp. 573–582, 2016

DOI: 10.3311/PPci.8605

Creative Commons Attribution ©

RESEARCH ARTICLE

Received 24-09-2015, revised 04-01-2016, accepted 12-01-2016

## Abstract

Impact of missiles into reinforced concrete structures can have various effects. Soft impacts (deformation of missile is more significant than deformation of target structure) might cause global failure, while hard impacts of quasi-rigid missiles only affect the impact zone and cause local failure such as cracks, penetration, perforation, etc. In our paper, local effects caused by hard missiles are examined. Missile parameters are close to possible primary and secondary missiles induced by tornados and aircraft impacts. Potential modelling and calculation methods are summarized and a calibrated FE model is presented. Based on FE model calculations, new semi-empirical formulae are deduced that can be applied for medium size hard missile impacts.

## Keywords

impact local effects · hard impact · penetration · perforation

## 1 Introduction

Impact of a hard (non-deformable) missile may have various effects on a concrete target. Usually local effects are dominant, such as penetration, cone cracking, crack formation, spalling, scabbing or perforation (Fig. 1).

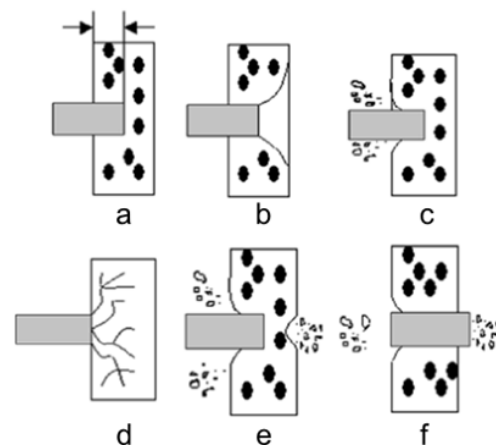


**Fig. 1.** Local effects of missile impact on concrete target: (a) penetration, (b) cone cracking, (c) spalling, (d) crack formation, (e) scabbing, (f) perforation [1]

Required resistance of a concrete wall depends on its protective function. Usually, perforation and secondary projectile formation have to be prevented, but for protected spaces with special functions (e.g. nuclear power plant (NPP) containments) effects on the distal side have to be excluded, too. The most important parameters that influence the effect of a hard missile impact are the velocity ( $V$ ), mass ( $m$ ), diameter ( $d$ ), nose shape ( $N$ ) of the missile, and thickness ( $t$ ), tensile and compressive strength ( $f_t, f_c$ ), reinforcement of the target. The most important quantities that characterize the impact are the penetration depth ( $x$ ), perforation limit ( $e$ ) and scabbing limit ( $s$ ). Perforation and scabbing limits are the minimum needed thicknesses to prevent perforation or scabbing, respectively.

At first, possible analysis methods, tests and models are summarized. Then a chosen numerical model is introduced that is calibrated to a well-known real experiment. Moreover, a parametric study is presented and the results are compared to the results of the most important formulae for penetration and per-

## Lili Eszter Laczák

Department of Structural Engineering, Faculty of Civil Engineering, Budapest University of Technology and Economics, H-1521 Budapest, P.O.B. 91., Hungary  
e-mail: laczak.lili@epito.bme.hu

## György Károlyi

Institute of Nuclear Techniques, Faculty of Natural Sciences, Budapest University of Technology and Economics, H-1521 Budapest, P.O.B. 91., Hungary  
e-mail: karolyi@reak.bme.hu

formation. New empirical formulae are also introduced that fit to the numerical model results.

## 2 Analysis methods

There are three main types of methods to analyse a hard impact and estimate its consequences: analytic, semi-empirical and empirical calculations. Since the beginning of the 20<sup>th</sup> century, tests also have been carried out to examine the behaviour of real structures. At first, high velocity impact tests of small missiles (military missiles, bullets) were carried out [2]. Examination of relatively lower velocity impacts of larger missiles (tornado generated missiles, accidental aircraft turbine impact, etc.) became important when construction of large number of NPPs started. Most of the calculation methods and formulae neglect missile deformation, effect of reinforcement, elastic target deformation etc. Penetration models usually assume the target to be a half-space and calculate penetration depth  $x$  without taking into account the thickness of the target.

### 2.1 Analytic and empirical methods

The first analytic models to calculate penetration aimed to determine the force that acts on the target during penetration and compared it to the resistance of the structure ( $F_p$ ). Kennedy [2] and Poncelet [3] assume that the resistance is a polynomial function of the velocity of impact, while the National Defense Research Council (NDRC) formula [2] writes it as the product of two functions:

$$F_p = g\left(\frac{x'}{d}\right) \cdot f(v) \quad , \quad (1)$$

where  $g$  depends on the ratio of the actual penetration depth  $x'$  to missile diameter  $d$  and  $f$  depends on the actual missile velocity  $v$ . Haldar [4] and Hughes [5] write penetration depth  $x$  as a function of a dimensionless impact factor ( $I$ ):

$$\frac{x}{d} = g(I) \quad , \quad (2)$$

$$I = \frac{m \cdot v^2}{f \cdot d^3} \quad . \quad (3)$$

Analytic perforation calculations usually assume that perforation occurs because of shear cone formation. After certain penetration the thickness of the target reaches a critical value ( $H$ ) and cone failure and perforation occur (Fig. 2.).

In such a multi-phase model, relative perforation limit ( $e/d$ ) can be calculated as:

$$\frac{e}{d} = \frac{x}{d} + \frac{H}{d} \quad , \quad (4)$$

where  $H$  depends on the target and missile properties. Li, Tong [6] and the UK Atomic Energy Authority (UKAEA) [7] used such multi-phase models in their calculations.

Parallel to the development of analytic formulae, several tests have been carried out to help the modelling of local failure.

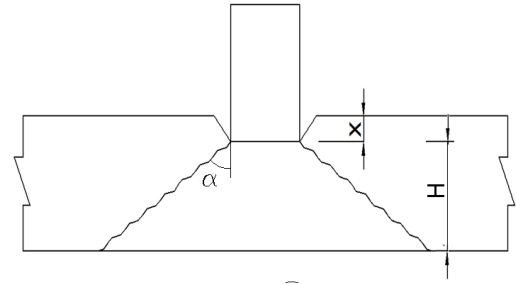


**Fig. 2.** Penetration followed by perforation (shear cone failure) [5]. The figure shows the situation when the perforation just occurs, in this limiting case the whole thickness  $t$  coincides with the perforation limit.

Based on the test results, empirical formulae were invented. Limits of applicability of these formulae highly depend on the original experiment. Medium and larger scale tests were done by Rüdiger and Riech [8], Kojima [9] and Sugano [10, 11].

### 2.2 Summarizing articles

The most important summarizing articles on local failure calculations were published by Li [1], Kennedy [2], Teland [12], and Murthy [13]. In these papers, the most important formulae are collected, compared and the results are analysed. The formulae used in the following chapters are mainly taken from these summarizing papers.

### 2.3 Numerical models

Due to the rapid development of finite element (FE) and discrete element (DE) methods, virtual experiments have become a powerful tool for impact problem calculations. The most problematic parts of these models are the material model of the concrete target and the contact problem handling. Resistance of concrete material highly depends on the impact velocity, therefore rate dependent material properties are required. Behaviour of concrete is usually modelled by a multi-stage material model that consists of a state equation (compaction model) that corresponds to the hydrostatic stress stage and a yield and failure surface in the deviatoric stress space. The yield surface (that has a hydrostatic stress dependent and independent component) models the post-elastic hardening region, while the failure (limit) surface sets the beginning of strain-softening. Compacted elements can still have a lower residual strength, modelled by the residual strength surface [14] (Fig. 3, Fig. 4).

The model also has to follow the different behaviour of concrete under tension and compression. Crack propagation can be modelled by fixed crack propagation (crack direction is pre-determined), arbitrary crack propagation (mesh-free methods, DE model) or a continuous material parameter modification (smeared crack model) [15]. Hard impact of larger missiles was simulated by various numerical techniques by Itoh [16], Mizuno [17], Cox [18], Lepannen [19], Shiu [20], Heckötter [21] and others.

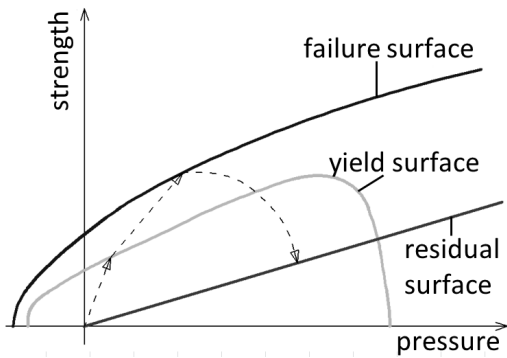


Fig. 3. Stress surfaces along the compression meridian [14]

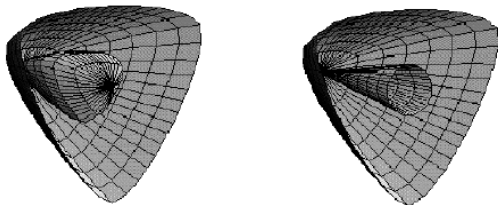


Fig. 4. Failure and residual surfaces (left), failure and elastic limit surfaces (right) in 3D [14]

### 2.4 Sugano experiment

One of the best documented multi-scale test series was executed by Sugano and his team [10, 11]. They used flat-nose, cylindrical, hard and semi-hard models of a GE J-79 military jet engine in three different scales (1/7.5, 1/2.5, 1/1) and concrete target plates with different size, thickness and reinforcement. In this paper we only focus on perfectly hard missiles therefore result of hard 1/7.5 and 1/2.5 scale experiments are used. Properties of hard missiles used by Sugano are summarized in Table 1.

During the experiments penetration depth, perforation limit and level of scabbing were registered.

## 3 FE model calibration

### 3.1 Geometry and material model

Our model is created in Ansys Workbench Explicit Dynamics explicit FE program. Contrary to the Sugano test's flat-nose missile, the FE model consists of cylinders with spherical nose that have the same length and mass as the Sugano missiles. Spherical nose is used for convergence reasons. In order to reduce computation time, a quarter-model with symmetry is used and the size of the target is reduced to the smallest possible size to prevent effect of boundaries (Fig. 5).

Reinforcement is not modeled at this stage, because according to test results [10, 11], it hardly affects the perforation and penetration properties (in case of high velocity impacts and normal amount of reinforcement). Material model is CONC-35MPa explicit material model of Ansys Workbench Explicit that includes the RHT strength model [14] that describes rate-dependent elastic limit, failure and residual surfaces, and also includes state equations for pressure dependence of compression and density. The built-in values of parameters are used, only compressive and tensile strain rate exponents were changed to 0.1 accord-

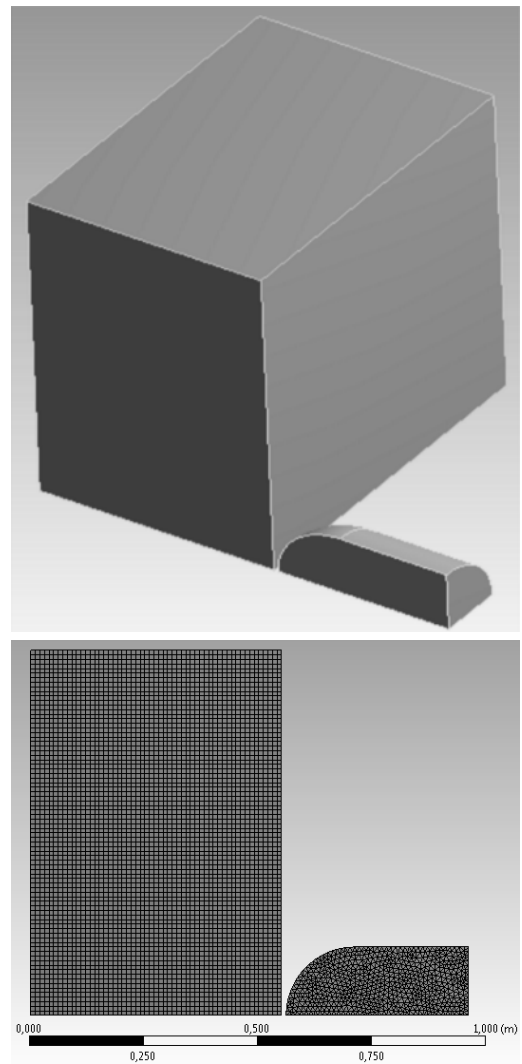


Fig. 5. FE model of target and missile

ing to the recommendation of Tu [22]. The material model fixes the tensile and compressive strength ratio and the shear and compressive strength ratio, therefore tensile and shear strength change if  $f$  changes. In the Sugano test, planned compressive strength of concrete was 23.5 MPa, but finally they measured higher strength values. The type of tested specimen was not described, therefore, during calibration,  $f$  turned out to be 40 MPa for 1/7.5 test and 45 MPa for 1/2.5 tests in our model. Finite element size dependency was examined and the applied size was calibrated to the real test results.

### 3.2 Results of calibration

Table 2 compares the results of the Sugano test to our FE model. In the table, penetration depth values of the Sugano test results are modified because of the nose-shape difference. Nose shape multiplying factor ( $N$ ) for flat nose is 0.72, while for blunt nose it is 0.84 [11], therefore original Sugano test penetration values are multiplied by  $0.84/0.72 = 1.17$ . The first three rows are the result of 1/7.5 scale tests, while the last three correspond to the 1/2.5 scale tests.

It can be seen that penetration depth results and perforation

**Tab. 1.** Properties of hard Sugano test missiles

Scale	1/7.5	1/2.5
mass	3.6 kg	100 kg
diameter	101 mm	300 mm
length	110 mm	400 mm
planned impact velocity	100, 150, 215 m/s	100, 150, 215 m/s

**Tab. 2.** Properties of hard Sugano test missiles

V [m/s]	t [mm]	f [MPa]	x [mm] Sugano*	x [mm] FEM	scabbing [mm×mm] Sugano	scabbing [mm×mm] FEM
200-220 (210)	350	23.5 (40**)	47	49	-	cracks
	180		perf.	59	260 × 260	610 × 675
	150		perf.	perf.	200 × 200	660 × 880
	600	23.5 (45**)	140	150	360 × 360	130 × 120
	550		146	perf.	400 × 400	200 × 150
	450		perf.	perf.	400 × 400	240 × 220

\*corrected results that take into account the nose-shape factor (see main text)

\*\*modified strength in FE model (see main text)

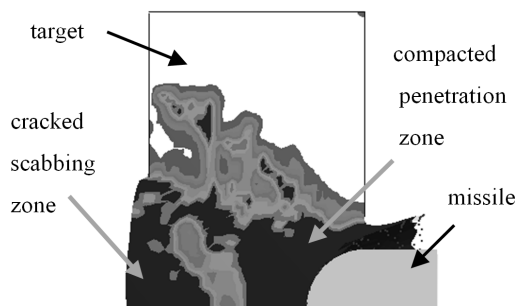


**Fig. 6.** Damage of 180 mm thick target

limits of the FE model agree well with real test results. The 180 mm thick target is the only case where perforation occurred in the real test, but did not occur in the FE model. However, Fig. 6 shows the result of the FE model of this case, the darkness of colours shows the level of damage in the target material, black colour represents the totally damaged elements. It is visible that on the proximal side the impact causes penetration and compaction, while on the distal side the reflection of shock waves causes scabbing. If the two fully damaged zones merge then perforation happens. In Fig. 6 it is visible that the two zones are close and thus the target is nearly perforated, thus practically the 180 mm target thickness case is also modelled quite adequately.

For the 550 mm thick target, corrected Sugano test result is 146 mm penetration, while FE model predicts perforation. In this case, the exact perforation limits of the real specimens and the level of damage in the not perforated zone is not available from the experiments, hence the measured and the FE results cannot be compared directly.

Scabbing zone sizes of the real experiment and the FE model are probably different because we neglect the reinforcement in the FE simulation. Contrary to perforation and penetration, scabbing can be affected by the reinforcement because it holds

together the damaged, cracked zone at the distal side.

#### 4 Parametric study

After the FE model calibration, a parametric study is carried out. The most important parameters that appear in the model (impact velocity, mass and diameter of the missile, concrete strength) are varied in a wide range of values. In the following diagrams, results of different empirical and analytic formulae are represented together with the numerical and Sugano test results. Only those formulae appear on the graphs that have results close to the results of the tests. Relative penetration depth ( $x/d$ ) and relative perforation limit ( $e/d$ ) values of the 1/7.5 and 1/2.5 tests are shown. On each graph, only one parameter is changed while all the other parameters are kept at the basic values used in the tests.

##### 4.1 Penetration and perforation (1/7.5 scale test)

Figs. 7 - 10 represent the relative penetration depth values of the 1/7.5 (S 1/7.5) tests as a function of missile and target parameters. Results of the UKAEA (UK Atomic Energy Authority), Adeli-Amin, Hughes, TBAA (British Textbook of Air An-nament) and Li formulae [1, 2, 12, 13] are also shown as well as the original and corrected Sugano test results. It is visible that the different formulae fit differently to the test results. The Hughes formula and TBAA formula fit quite well to the FE model results, however, usually give higher  $x/d$  values than the FE model. Adeli-Amin and UKAEA formulae overestimate, while the Li formula underestimates the FE results. In all the graphs, the dashed-dotted line shows the result of a new semi-empirical formula fitted to the FE model results. This new formula is detailed in Section 5.

Figs. 11 - 14 show the relative perforation limit values of the 1/7.5 test together with the results of the Hughes, Chang, CEA

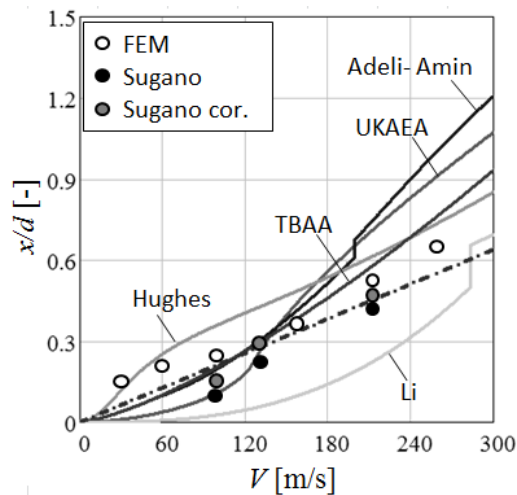


Fig. 7. Relative penetration depth — velocity curve (S 1/7.5)

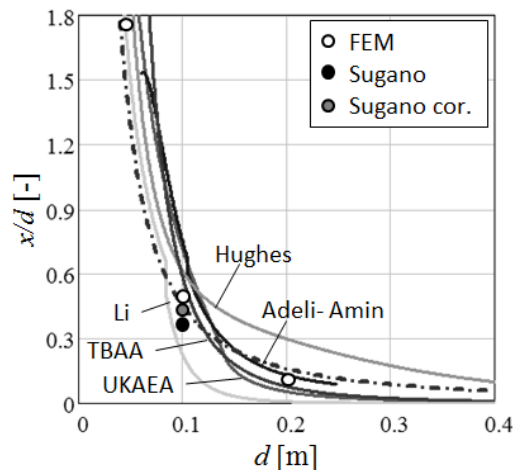


Fig. 9. Relative penetration depth — missile diameter curve (S 1/7.5)

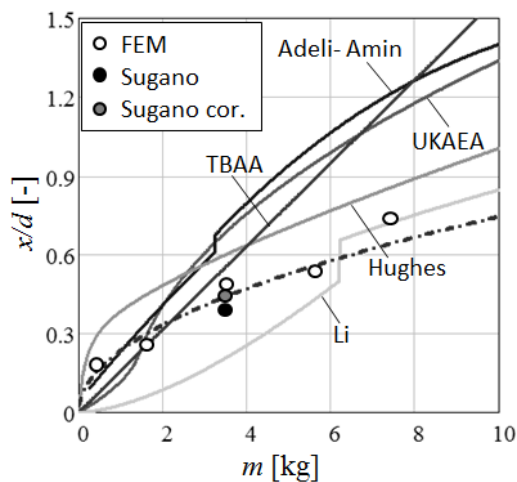


Fig. 8. Relative penetration depth — missile mass curve (S 1/7.5)

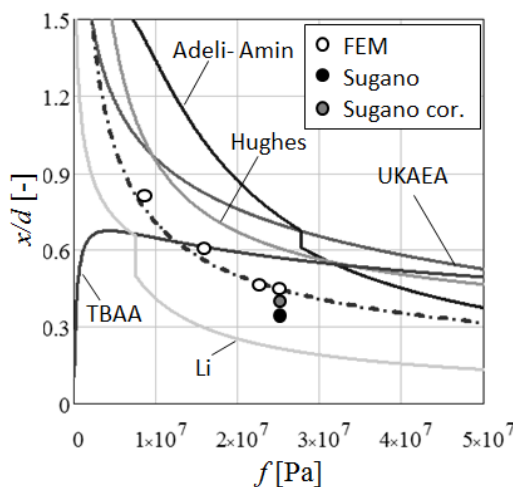


Fig. 10. Relative penetration depth — concrete strength curve (S 1/7.5)

(French Atomic Energy and Alternative Energies Commission), Criepi formulae [1, 2, 12, 13]. Criepi and CEA formulae results are in good agreement with the FE model results, Hughes formula moderately, and Chang formula significantly overestimates them. Penetration depth values vary between 2 - 8 cm ( $x/d \sim 0.2 - 0.8$ ), basic Sugano test value is 4.7 cm ( $x/d = 0.47$ ), while perforation limits are between 10 - 30 cm ( $e/d \sim 1 - 3$ ) and Sugano test limit value is around 18 cm ( $e/d = 1.8$ ).

#### 4.2 Penetration and perforation (1/2.5 scale test)

Relative penetration depth values of the 1/2.5 scale tests can be seen on Figs. 15-18 together with the result obtained from the UKAEA, TBAA, Adeli-Amin, Hughes and NDRC formulae. Figs. 19-22 represent perforation limit curves of FE, Chang, Hughes, CEA, Criepi models. In some cases, convergence problems occurred in the FE model, mainly when low density or low velocity impacts were simulated, therefore less FE results appear in the graphs than in case of the 1/7.5 tests.

Based on Figs. 15-18, penetration values of the Hughes formula are the closest to the FE model results. TBAA, UKAEA and Adeli-Amin formula results are significantly higher and Li formula results are lower than the FE model  $x$  values. In case

of the penetration limit calculations, similarly to the 1/7.5 test results, Criepi and CEA formulae results are in good agreement with the FE model, Hughes formula moderately, and Chang formula significantly overestimates the results.

Compared to the smaller missile test results, both penetration depths and perforation limits are much bigger in the 1/2.5 test case. Penetration values are between 1 - 30 cm ( $x/d \sim 0.03 - 1.0$ ) in the FE model, Sugano test result was 14 cm ( $x/d = 0.47$ ). FE model perforation limit values are between 20 - 80 cm ( $e/d \sim 0.6 - 2.6$ ), while 45-55 cm in the Sugano test ( $e/d \sim 1.5 - 1.8$ ).

Size effect is not significant: basic case  $x/d$  and  $e/d$  values of the 1/7.5 test are 0.49 and 1.7, while 0.44 and 1.9 in the 1/2.5 test.

### 5 New empirical formulae

New dimensionless empirical formulae are fitted to the results of our FE model. Figs. 23 - 24 show the results of Sugano and FE tests as a function of the dimensionless impact factor of Eq. (3) in a log-log scale coordinate system, the fitted formulae for  $x/d$  and  $e/d$  are also represented.

It is visible that all FE and experimental data more or less fall on a single curve, indicating that both  $x/d$  and  $e/d$  indeed de-

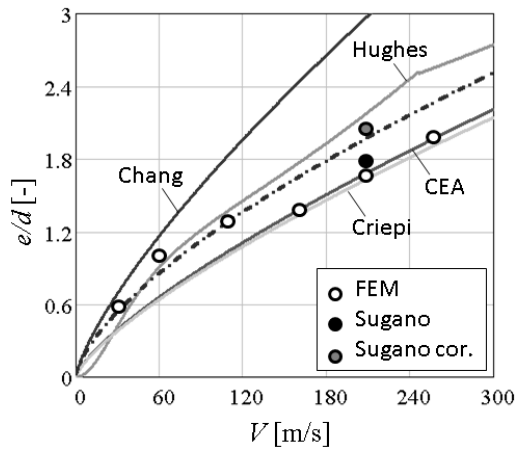


Fig. 11. Relative perforation limit—velocity curve (S 1/7.5)

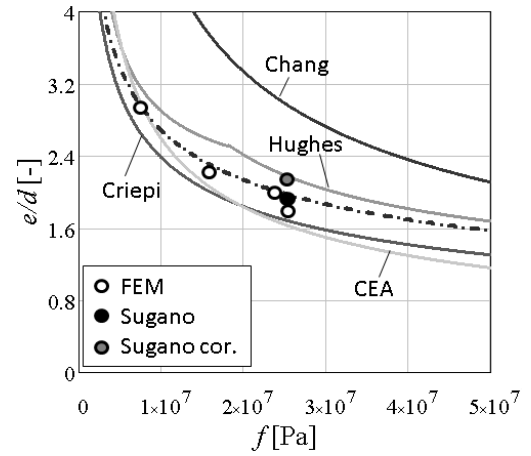


Fig. 14. Relative perforation limit—concrete strength curve (S 1/7.5)

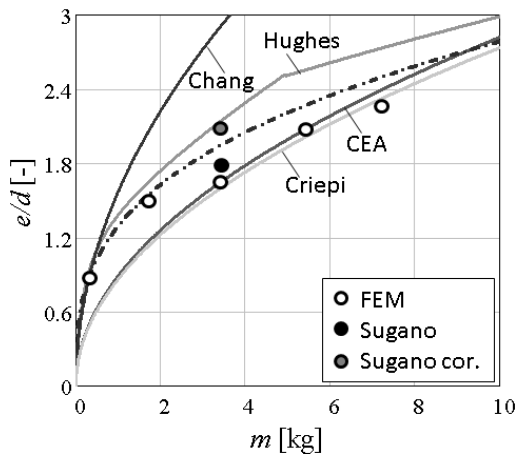


Fig. 12. Relative perforation limit—missile mass curve (S 1/7.5)

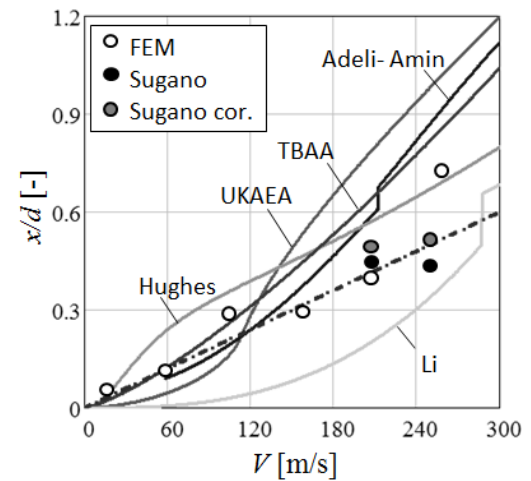


Fig. 15. Relative penetration depth—velocity curve (S 1/2.5)

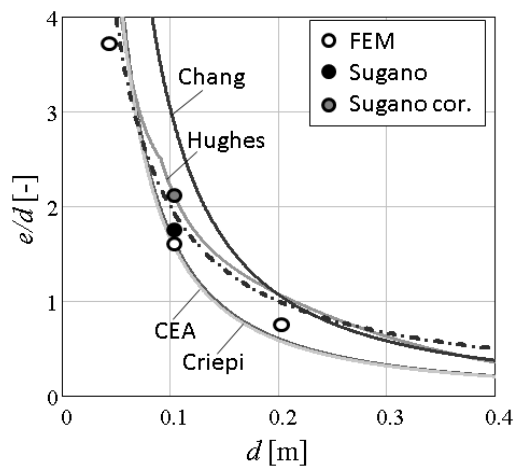


Fig. 13. Relative perforation limit—missile diameter curve (S 1/7.5)

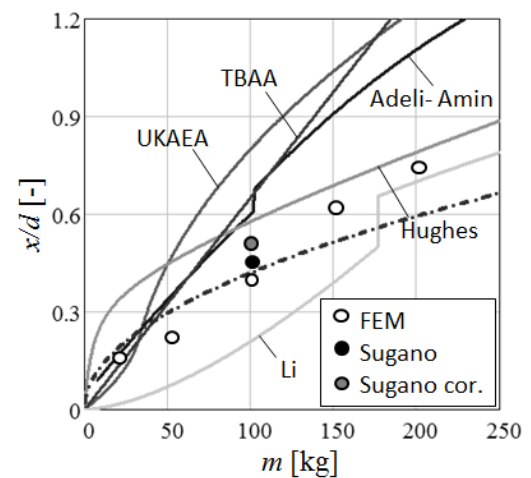


Fig. 16. Relative penetration depth—missile mass curve (S 1/2.5)

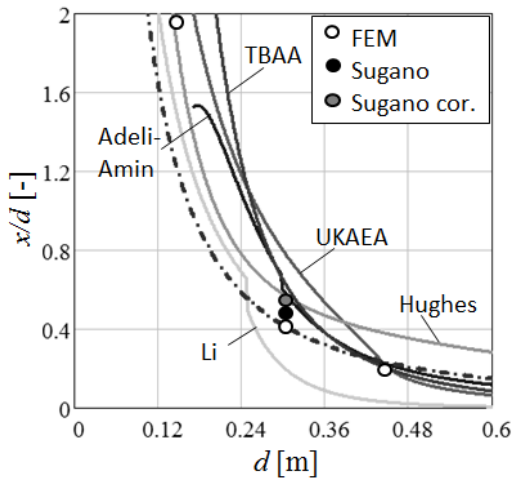


Fig. 17. Relative penetration depth — missile diameter curve (S1/2.5)

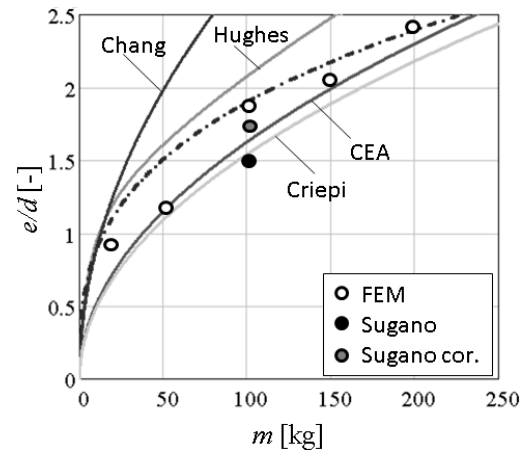


Fig. 20. Relative perforation limit — missile mass curve (S1/2.5)

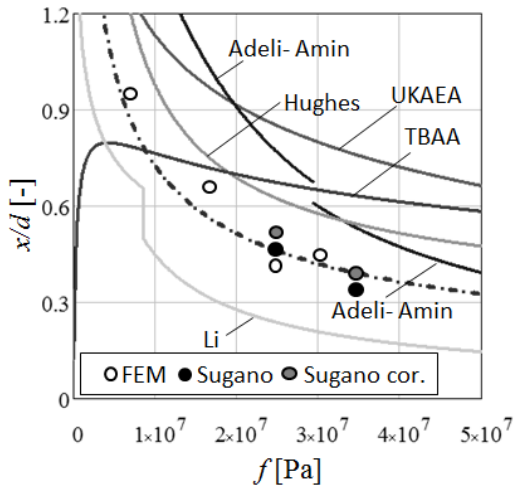


Fig. 18. Relative penetration depth — concrete strength curve (S1/2.5)

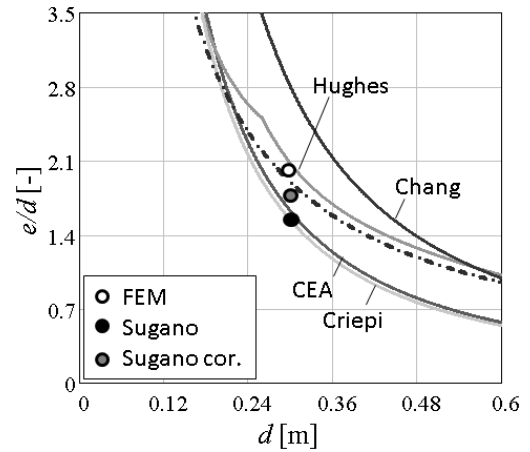


Fig. 21. Relative perforation limit — missile diameter curve (S1/2.5)

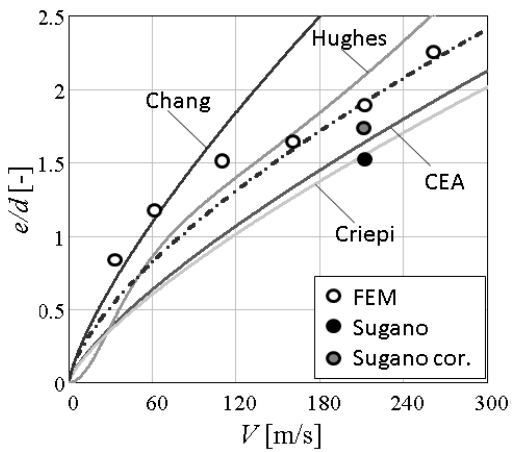


Fig. 19. Relative perforation limit — velocity curve (S1/2.5)

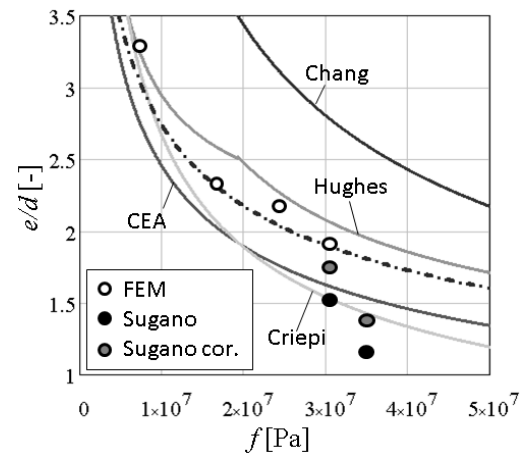
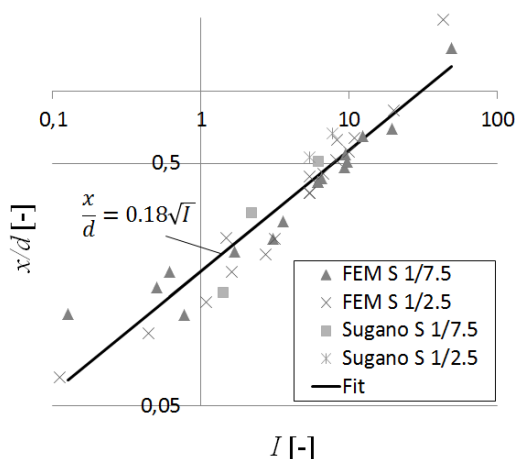


Fig. 22. Relative perforation limit — concrete strength curve (S1/2.5)

pend on the impact factor, which is a dimensionless combination of the parameters. This is not surprising, as this combination is the only dimensionless quantity that can be constructed from  $m$ ,  $V$ ,  $f$  and  $d$ , the parameters that determine the outcome of the impact. That all data points fit quite well to a straight line on the log-log diagrams shown in Figs. 23 and 24 indicates that there is a power law dependence of both  $x/d$  and  $e/d$  on  $I$ . We find that the exponent is close to 1/2 in case of  $x/d$  and 1/3 in case of  $e/d$ . The fitted formulae are the following:

$$\frac{x}{d} = 0.18 \sqrt{I}, \quad (5)$$

$$\frac{e}{d} = 1.08 \sqrt[3]{I}. \quad (6)$$



**Fig. 23.** Relative penetration as a function of the impact factor (log-log graph)

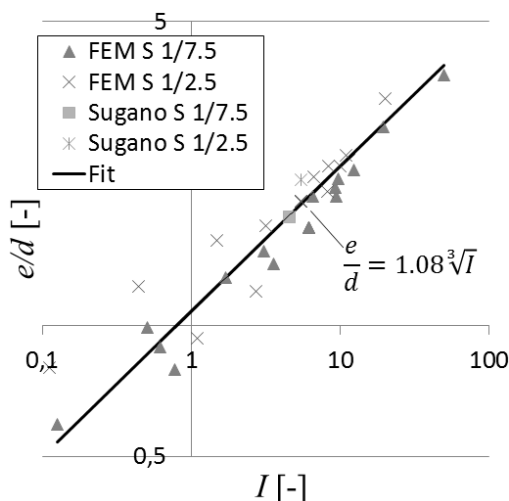


**Fig. 24.** Relative perforation limit as a function of the impact factor (log-log graph)

The fitted functions are represented in Figs. 7-22 by dashed-dotted lines. Table 3 shows the absolute and relative mean deviation of our formula from the FE model results. Relative deviation is 14-16% in case of penetration values and 10-12% in case of perforation limit values.

The simple power law we found indicates that there is a simple physical connection between the penetration or perforation

and the ratio of the impact energy  $1/2 mV^2$  to the resistance of the target  $fd^2$ . In the following we give a possible explanation of this result. Fig. 25 represents the penetration ( $x$ )—resistance ( $F$ ) function as proposed by Hughes [5]. According to the Hughes model, if the penetration is small enough compared to the target thickness then penetration resistance will be similar to the resistance of an infinite half space. In this case, penetration resistance linearly increases with penetration depth until a critical penetration depth  $x_1$  is reached:

$$F(x) = kx, \quad x \leq x_1. \quad (7)$$

If we assume that missile kinetic energy causes penetration then:

$$\frac{1}{2}mV^2 = \int_0^x F(x)dx = \frac{1}{2}kx^2, \quad (8)$$

therefore  $x$  is proportional to the square root of the kinetic energy:

$$x = \sqrt{\frac{mV^2}{k}} \quad (9)$$

therefore

$$\frac{x}{d} = \sqrt{\frac{df}{k}} \sqrt{I}, \quad (10)$$

which gives the same square root dependence of  $x/d$  in the impact factor  $I$ .

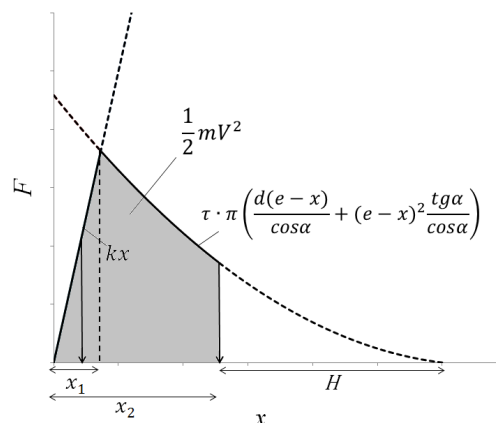


**Fig. 25.** Resistance – penetration depth function based on Hughes model [5]

If  $x > x_1$ , then the finite thickness of the target starts to affect the resistance, the resistance decreases due to the decrease of the undamaged thickness ( $t - x$ ). The resistance at this decreasing phase assumed to be equal to the resistance against shear cone failure (see Fig. 2) that has the following form:

$$F(x) = \tau A = \tau \pi \left( \frac{d(t-x)}{\cos \alpha} + (t-x)^2 \frac{tg \alpha}{\cos \alpha} \right), \quad x > x_1, \quad (11)$$

where  $\tau$  is the shear strength of the target, that is a function of the strength  $f$ ,  $A$  is the lateral surface area of the shear cone

**Tab. 3.** Mean deviation

S1/7.5			
x		e	
abs. [mm]	rel.	abs. [mm]	rel.
4,65	14,50%	15,48	10,77%
S1/2.5			
x		e	
abs. [mm]	rel.	abs. [mm]	rel.
18,02	15,91%	50,60	11,49%

and  $\alpha$  is the shear cone angle (Fig. 2). If the undamaged thickness reaches the critical value  $H$  then resistance drops down to 0 and perforation occurs. If  $t = e$ , i.e. when perforation occurs no residual kinetic energy remains. We assume that perforation occurs when a given portion of the thickness is penetrated, so penetration depth  $x_2$  is proportional to  $e$ :

$$x_2 = e - H = \beta e. \quad (12)$$

If we neglect the linearly increasing first part as suggested by Hughes [5] and write down the kinetic energy consumption of penetration, then we obtain

$$\frac{1}{2}mV^2 = \int_0^{x_2} F(x)dx = \int_0^{\beta e} \tau\pi \left( \frac{d(e-x)}{\cos\alpha} + (e-x)^2 \frac{tg\alpha}{\cos\alpha} \right) dx. \quad (13)$$

Performing the integration, we find  $e^3$  on the right-hand side, which implies that  $1/2mV^2$ , and hence  $I$  are a cubic function of  $e$ . This is what we obtained in Eq. (6).

## 6 Conclusions

In our paper, new semi-empirical formulae for penetration and perforation caused by hard impact are introduced. It is based on calibrated FE model calculations. The calculation neglects the effect of reinforcement and missile deformation, but includes the study of a wide range of parameters. The most important parameters of hard impact into concrete structure (missile size, mass, impact velocity, concrete strength) are examined and an excellent agreement with our new formulae is found. The formulae are based on numerical tests, therefore their applicability has limits, but our formulae seem to be applicable for smaller and medium size hard missiles (with mass of 0,5 - 200 kg) that impact with 50 - 300 m/s velocity. The examined parameter range contains the usual parameter values of tornado and aircraft impact generated hard missiles. We also present a simple heuristic theoretical model that supports our new formulae.

## Acknowledgement

The project presented in this article is supported by OTKA no. K 100894, Paks NPP and JNEA (Foundation for Nuclear Engineers).

## References

- 1 **Li QM, Reid SR, Wen HM, Telford AR**, *Local impact effects of hard missiles on concrete targets*, International Journal of Impact Engineering, **32**, (2005), 224–284, DOI 10.1016/j.ijimpeng.2005.04.005.
- 2 **Kennedy RP**, *A review of procedures for the analysis and design of concrete structures to resist missile impact effects*, Nuclear Engineering and Design, **37**, (1976), 183–203, DOI 10.1016/0029-5493(76)90015-7.
- 3 **Poncelet JV**, *Introduction a la mecanique industrielle (Introduction to industrial mechanics)*, Gauthier-Villars; Paris, 1829.
- 4 **Haldar A, Hamieh HA**, *Local effects of solid missiles on concrete structures*, ASCE Journal of Structural Engineering, **110**, (1984), 948–960, DOI 10.1061/(ASCE)0733-9445(1984)110:5(948).
- 5 **Hughes G**, *Hard missile impact on reinforced concrete*, Nuclear Engineering and Design, **77**, (1984), 23–35, DOI 10.1016/0029-5493(84)90058-X.
- 6 **Li QM, Tong DJ**, *Perforation thickness and ballistic limit of concrete target subjected to rigid projectile impact*, ASCE Journal of Structural Engineering, **129**, (2003), 1083–1091, DOI 10.1061/(ASCE)0733-9399(2003)129:9(1083).
- 7 **Li QM, Chen XW**, *Dimensionless formulae for penetration depth of concrete target impacted by a nondeformable projectile*, ASCE Journal of Engineering Mechanics, **28**, (2003), 93–116, DOI 10.1016/S0734-743X(02)00037-4.
- 8 **Rudiger E, Riech H**, *Experimental and theoretical investigations on the impact of deformable missiles onto reinforced concrete slabs*, In: Proceedings of 7th International Conference on Mechanics in Reactor Technology (SMiRT), International Association for Structural Mechanics in Reactor Technology, 1983, pp. 387–394.
- 9 **Kojima I**, *An experimental study on local behavior of reinforced concrete slabs to missile impact*, Nuclear Engineering and Design, **130**, (1991), 121–132, DOI 10.1016/0029-5493(91)90121-W.
- 10 **Sugano T, Tsubota H, Kasai Y, Koshika N, Ohnuma H, Riesenmann WA, Bickel DC, Parks MB**, *Local damage to reinforced concrete structures caused by impact of aircraft engine missiles Part 1. Test program, method and results*, Nuclear Engineering and Design, **140**, (1993), 387–405, DOI 10.1016/0029-5493(93)90120-X.
- 11 **Sugano T, Tsubota H, Kasai Y, Koshika N, Ohnuma H, Riesenmann WA, Bickel DC, Parks MB**, *Local damage to reinforced concrete structures caused by impact of aircraft engine missiles Part 2. Evaluation of test results*, Nuclear Engineering and Design, **140**, (1993), 407–423, DOI 10.1016/0029-5493(93)90121-O.
- 12 **Teland JA**, *A review of empirical equations for missile impact effects on concrete. Report no. FFI/RAPPORT-97/05856*, Norwegian Defence Research Establishment, 1998, www.ffi.no/no/Rapporter/97-05856.pdf.
- 13 **Murthy ARC, Palani GS, Iyer NR**, *Impact Analysis of Concrete Structural Components*, Defense Science Journal, **60**, (2010), 307–319, DOI 10.14429/dsj.60.358.
- 14 **ANSYS Workbench Help, Version 15.0.0**, SAS IP Inc., 2013.
- 15 **Bojtar I**, *Toresmechanika, Egyetemi jegyzet, (Fracture mechanics, Lecture Notes*, Pal Vasarhelyi Doctoral School of Civil Engineering and Earth Sci-

ences, 2015. <https://www.me.bme.hu/hu/kurzus/toresmechanika>. (in Hungarian).

- 16 **Itoh M, Katayama M, Mitakes S, Niwa N, Beppu M, Ishikawa N**, *Numerical study on impulsive local damage of reinforced concrete structures by a sophisticated constitutive and failure model*, In: Proceedings of the SUSI VI: Structures Under Shock and Impact VI, WIT, 2001, pp. 569-578.
- 17 **Mizuno J, Sawamoto Y, Yamashita T, Koshika N, Niwa N, Suzuki A**, *Investigation on impact resistance of steel plate reinforced concrete barriers against aircraft impact. Part 1-3*, In: Proceedings of 18th International Conference on Mechanics in Reactor Technology (SMiRT), International Association for Structural Mechanics in Reactor Technology, 2005, pp. 2566-2579.
- 18 **Cox PA, Mathis J, Wilt T, Chowdhury A, Ghosh A**, *Assessment of structural robustness against aircraft impact at the potential repository at Yucca Mountain- Progress report, NRC-02-02-012*, Center for Nuclear Waste Regulatory Analyses, 2005, <http://pbadupws.nrc.gov/docs/ML0626/ML062620364.pdf>.
- 19 **Lepannen J**, *Concrete subjected to projectile and fragment impacts: Modelling of crack softening and strain rate dependency in tension*, International Journal of Impact Engineering, **32**, (2006), 1828–1841, DOI 10.1016/j.ijimpeng.2005.04.005.
- 20 **Shiu W, Donze F, Daudeville L**, *Discrete element modelling of missile impacts on reinforced concrete target*, International Journal of Computer Applications in Technology, **34**, (2009), 33-41, DOI 10.1504/IJCAT.2009.022700.
- 21 **Heckotter C, Sievers J, Tarallo F, Bourasseau N, Cire B, Saarenheimo A, Calonius K, Tuomala M**, *Comparative analyses of impact tests with reinforced concrete slabs*, Eurosafe Forum, 2010, [http://www.eurosafe-forum.org/sites/default/files/Eurosafe2010/1\\_02\\_IMPACT\\_TESTS.pdf](http://www.eurosafe-forum.org/sites/default/files/Eurosafe2010/1_02_IMPACT_TESTS.pdf).
- 22 **Tu Z, Lu Y**, *Modifications of RHT material model for improved numerical simulation of dynamic response of concrete*, International Journal of Impact Engineering, **37**, (2010), 1072-1082, DOI 10.1016/j.ijimpeng.2010.04.004.